

**Developing a novel DLC-based thermo-photo-betavoltaic device for
remote extensible energy conversion and storage**

Anna Du

Phillips Academy

Patent Pending: US Patent Application 63/251,552

Table of Contents

Abstract	3
Introduction	4
Material and Methods	12
Results	27
Discussion and Conclusions	29
References	32

Abstract

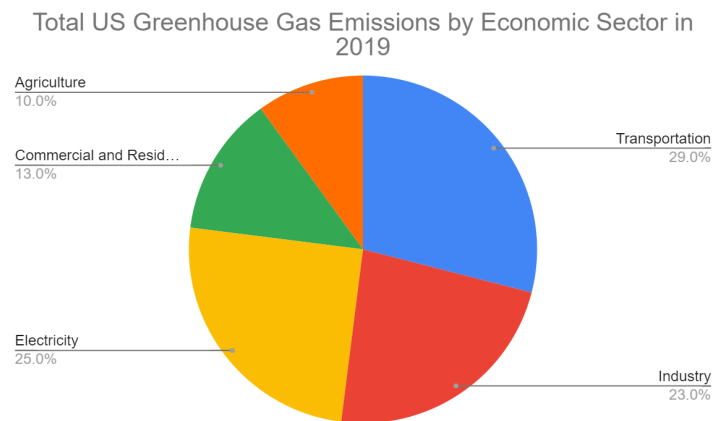
This patent-pending project is a high-efficiency energy production, conversion, and storage device, capable of utilizing the low costs and superlative thermal, semiconductive, and electrical properties of diamond-like carbon (DLC). Various stacked DLC configurations were attempted, through physical development and simulation modeling. The thermo-photo-betavoltaic energy conversion and storage device would be compact, long-lasting, and energy-efficient, able to be used in various environments, including remote locations and extreme environments. It is necessary to produce a more extensible range of power output, with higher current densities, and operational capabilities at higher voltages, to serve the ever-increasing needs of data-intensive computing operations, especially those in remote conditions. High sp³/sp² DLC is capable of superlative energy production using both heat and light, inherently possessing a wider bandgap potential (up to ~5eV. DLC). During use in field emission, applications have been shown to demonstrate superlative electron emission properties when exposed to a forward-bias voltage. As such, a novel design is being proposed, utilizing waste graphite nuclear rods with DLC coatings to maximize the potential for energy output, while reducing the global supply of nuclear waste. Additional related designs are also proposed, utilizing thermophotovoltaics (converting thermal energy and photons into electrical energy), and betavoltaics (which generates electricity through the constant emission of beta particles), to lessen the dependence on greenhouse gases. Various stacked DLC configurations, primarily based on P-N junction designs, were simulated, implemented, and tested, demonstrating a clear photoelectric and thermionic effect with up to ~100mV output tested, and a theoretical efficiency exceeding 25%, beyond today's photovoltaic.

Introduction

Currently, there is an environmental crisis across the globe. The temperature of the planet is increasing, and energy consumption continues to drive increases in pollution and socioeconomic inequities throughout the world. Yet people continue to be dependent on processes that require greenhouse gases (GHGs). A number of solutions have been proposed to alleviate this situation, including reductions within GHG emitting industries, and usage of more renewable energy sources by power companies, as well as electrification of the transportation industry, and more. At the same time, new technologies such as artificial intelligence, blockchain/crypto, cloud computing, and increased focus on data science and related technologies are using ever-increasing quantities of energy.

The retail world has rapidly increased its consumption of IoT devices, with AI natural language processing capabilities (Alexa, Siri, Google Assistant, etc. are expected to be a \$17.85B market by 2025, with a 26% CAGR). The commercial world has also increased its use of IoT in industry and even in green finance, using IoT devices to sense and report energy usage and other data for ESG reporting, and building management needs. The convergence of the AI industries and the IoT industries has led to a new paradigm known as AIOT, which is expected to connect an ever-increasing number of points of data, with the added benefits of machine learning, to help make this data collection ever more efficient. It is expected that the market for smart sensors will increase rapidly in the coming years. Given the remote nature of IoT and the fact that there are newer wireless capabilities (including 5G and new satellite technologies) emerging throughout the world, it is only a short matter of time before AIOT devices extend to the most remote locations on Earth, as well as throughout outer space.

There is a clear need for a novel energy production, conversion, and storage device, that is capable of extensible use in different environments, with the ability to use multiple energy input sources. Dynamic and remote environments have constantly changing temperature, light, pressure, and other conditions, and as such, the energy production/conversion/storage devices of the future must be capable of dynamic energy input from multiple sources, in a highly dense and compact form. As computing devices continue on their trend toward lower over time, the energy needs for mobile, wireless computing will fall within the range of betavoltaic and hybrid thermionic/photovoltaic devices (peak output efficiency of computers has doubled every 1.6 years, with a 100 fold increase in efficiency every decade).



This image shows the distribution of which industry uses the most electricity.

Currently, renewable energy is relatively expensive. Wind power is comparatively cost-effective, at around \$ 0.06 per kilowatt-hour. On the other hand, as of right now, solar power is one of the

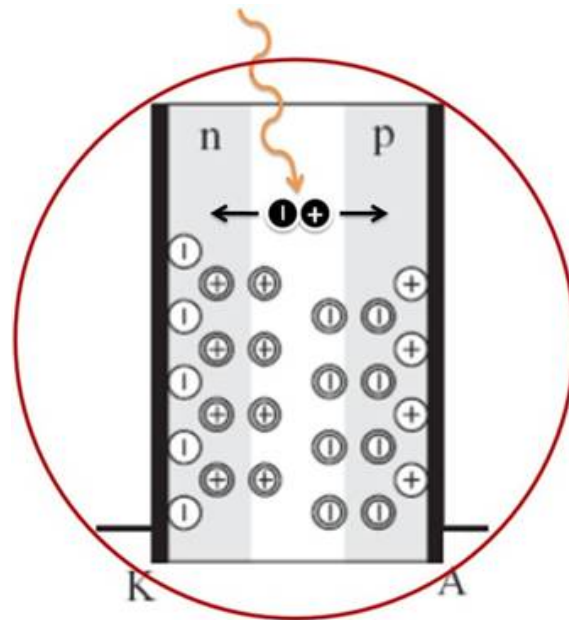
least cost-effective, costing around \$0.1 per kilowatt-hour. However, the cost of solar power is becoming more affordable as newer, more efficient solar cells are being created.

In the past few decades, coal, oil, and gas have been used the most, primarily due to their economic efficiency. This device utilizes a number of different sources of energy, including photovoltaics, betavoltaics, and thermionic emissions. Hopefully, by creating a thermo-photo-betavoltaic device, it would be possible to create an equally cost-efficient yet still effective energy source.

Photovoltaics is incredibly useful, and an abundant source of energy. There are around 173 terawatts of solar power on the surface of the Earth at one time, which is tens of thousands of times more than the total energy used in the world. Solar cells are typically made from silicon (although a number of materials are also being used/considered, silicon is by far the most common, especially as it is the second most abundant element on Earth). Typically, two types of silicon are used to form a p-n junction, which are boundaries that only allow electrons to flow through in a single direction (and are commonly used in diodes and transistors).

This p-n junction allows the solar cell to collect the energy, and potentially store it for later use. To form a p-n junction, p-type (a material that contains electron holes, and is therefore positively charged) and n-type (a material that contains an excess of electrons) silicons must be made. Due to the differences in the number of electrons that are in each type of material, when contact is made and the photons hit the solar cells, the excess electrons from the n-type silicon flow into the electron holes in the p-type silicon, and the center portion becomes the part where electrons can flow through. P-type silicon is typically made by doping the silicon with materials such as boron,

and n-type silicon is typically made by doping the silicon with materials such as phosphorus or arsenic. Doping is the introduction of impurities in a semiconductor crystal to allow the modulation of the optical, structural, and electrical properties of the semiconductor.

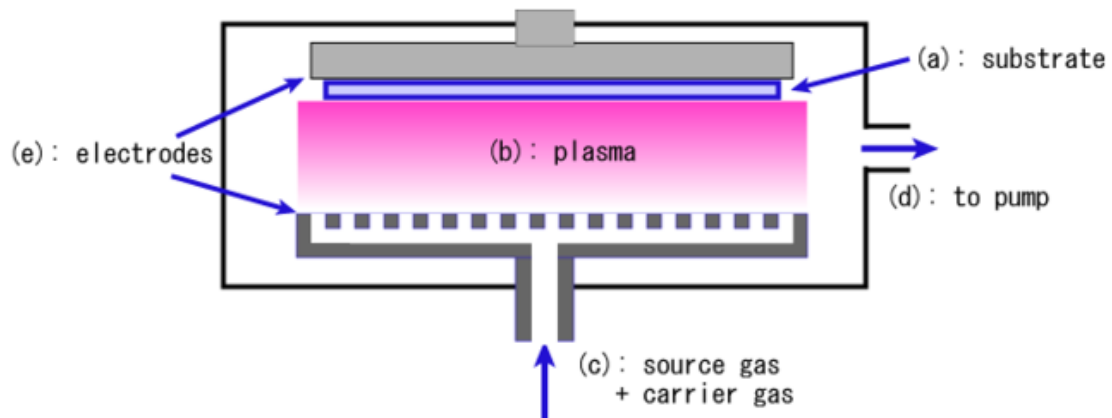


Betavoltaics is another form of energy that is proposed within this project. Beta radiation is the emission of a beta particle, which is a free electron, not attached to an atom (essentially ejected from the atom during beta decay). As with normal electrons, it has a small mass ($9.10938 \times 10^{-28} \text{g}$), and a negative charge. The movement of beta radiation is halted within a radius of six feet of air or roughly two millimeters of steel. As such, it is possible to encase betavoltaics within a heterogeneous material, encased by a sheet metal casing, and safely use it in an environment with proximity to human activity. Every year, over 250,000 tons of nuclear waste are produced, and improperly disposed of. One such waste is the graphite rods which are the control rods, which modulate the speed of the neutrons, and initiate fission when absorbed by the nucleus of a U-235

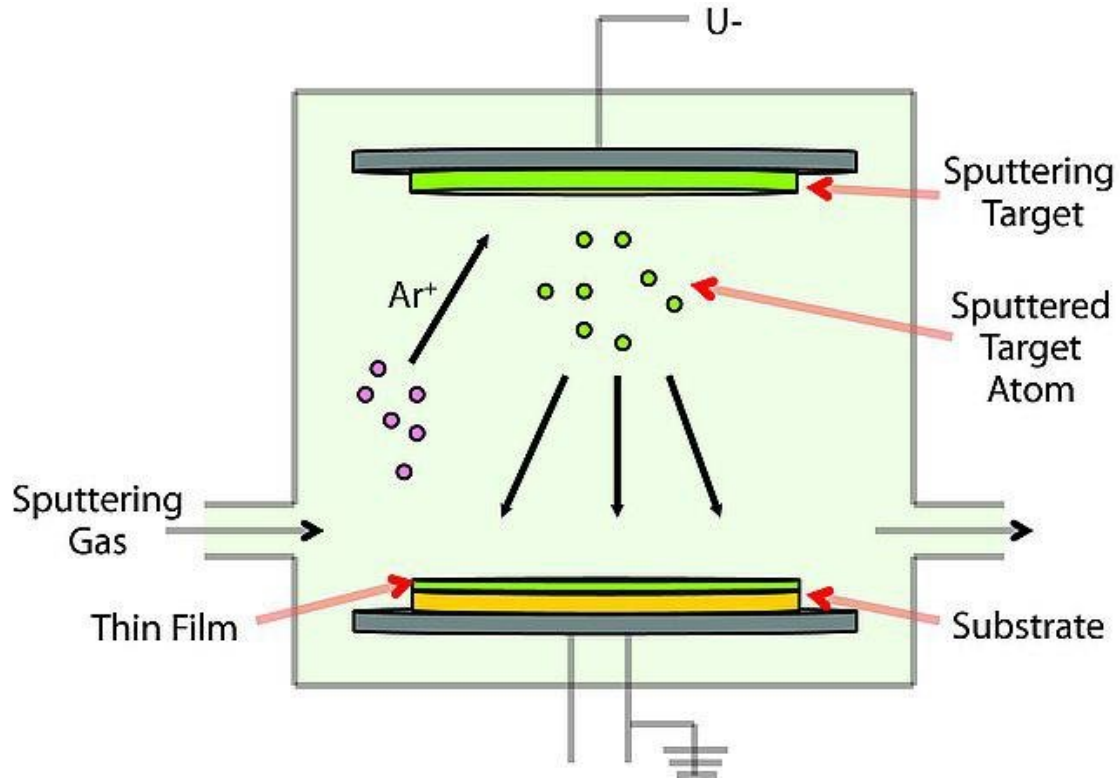
atom. When nuclear power plants are decommissioned, these graphite rods are filled with the radioactive isotope C-14, which has a half-life of 5,730 years.

Thermionic emission is the discharge of electrons from a heated material. The material in question can contain a p-n junction for the collection of the atoms. Thermoelectric materials generate electricity through the application of a temperature gradient. In some cases, this is done using the Seebeck effect, which occurs when the temperature difference between two electrically conducting materials allows a voltage difference to be produced. As the n-type material is heated up, the electrons tend to flow from the n-type to the p-type material, creating a flow, and thus producing electricity.

DLC (diamond-like carbon), or amorphous diamond, is a unique, low-cost, material that is comprised of a number of carbon species, including diamond, diamine, graphene, single-walled carbon nanotubes, buckminsterfullerene, and graphite. It is typically applied as a coating using a number of different technologies, most notably PVD and CVD (physical vapor deposition and chemical vapor deposition, respectively). Depending on the formula used to deposit DLC, the properties of the material can range from approximating graphite to approximating diamond. This can be roughly considered proportional to its sp^3 vs sp^2 bonding ratio, as determined by spectroscopy. Higher sp^3 bond levels, closer to diamond, are generally considered to be associated with more favorable materials. Due to this, there are many superlative properties of high sp^3/sp^2 ratio DLC, including its ability to emit electrons through a vacuum. There are a number of methods to deposit DLC onto a surface, including CVD (chemical vapor deposition), PVD (physical vapor deposition), and PE-PVD (plasma-enhanced physical vapor deposition).



CVD, comparatively, is thicker, more heat resistant, and is better on irregular surfaces as it coats evenly everywhere. Inside the reaction, the sample is heated up to 2000 degrees Celsius, and then mixed gasses are added, reacting when the gases make contact with the solid surface and are held on through localized attractions.



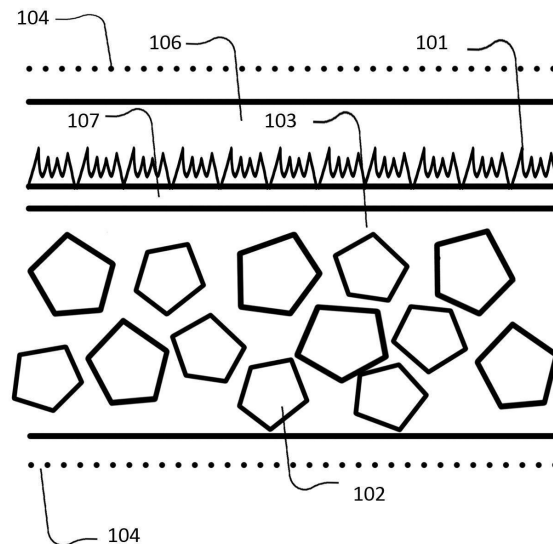
With PVD, the coating is line-of-sight only and is thinner and sharper. It's a much slower process, but the purity is very high. The material being coated is evaporated in a vacuum, and vapor travels to the substrate, deposits, and is condensed into a solid-state.

Diamond is known for its superlative properties such as being the most thermally conductive material on the planet, as well as the most electrically conductive (along crystal planes), and its ability to transmit both phonons and photons. It has only been in recent decades that the amazing properties of carbon-based materials have begun to be explored. Although some aspects of the thermionic, photoelectric, and field emission effects of diamond/DLC have been known since the mid-2000s, there has not been in-depth research on the use of DLC as a stacked PN multi-energy source power generation device. The benefits of using DLC are quite clear, as the broad range of bandgap potential, means that a range of output voltages can be achieved, with a maximum of

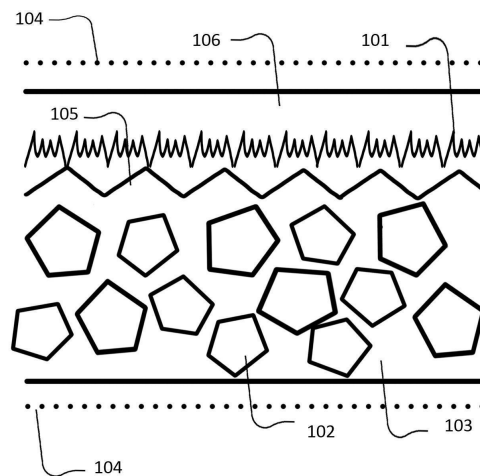
5V, which is far larger than most other Si-based devices can achieve. In the past several years, MIT scientists have theorized about the possibility of using C-14 diamonds in the form of a battery or energy storage device. Having conducted a patent search, it appears that the concept of a stacked DLC-based semiconductor device, using a betavoltaic source to act as a forward bias voltage to enhance the efficiency of the overall device, has not been explored. As such, a provisional patent has been filed in 2021, and a follow-up improvement application has also been filed in 2022.

Material and Methods

Numerous configurations for the device were designed, to account for a variety of plausible use cases, and to see which option would potentially output the most energy, under a range of different environmental conditions.

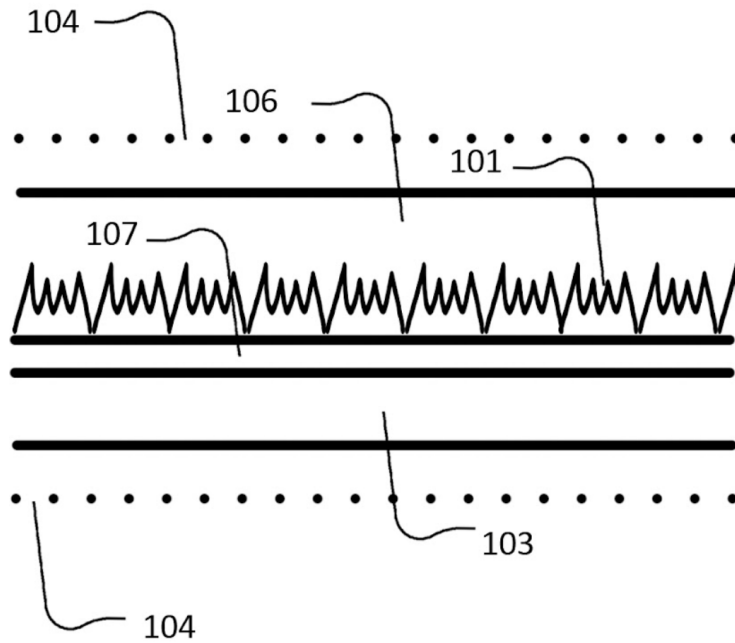


For this design, diamonds which are filled with C-14 (102) (perhaps recycled from graphite rod wastes from nuclear facilities), are used as the source of beta radiation and are embedded inside copper. This substrate is coated with a chromium interlayer (107) and DLC (101), with the chromium interlayer acting as a layer that allows for better adhesion and maximizes the points of contact between the DLC and copper, and prevents heat expansion from causing cracks in the DLC. The electrons are emitted from the DLC to reach the electron collection plate (104), and the spaces in between are filled with either a vacuum or a dielectric (106) depending on the pressure of the environment outside.

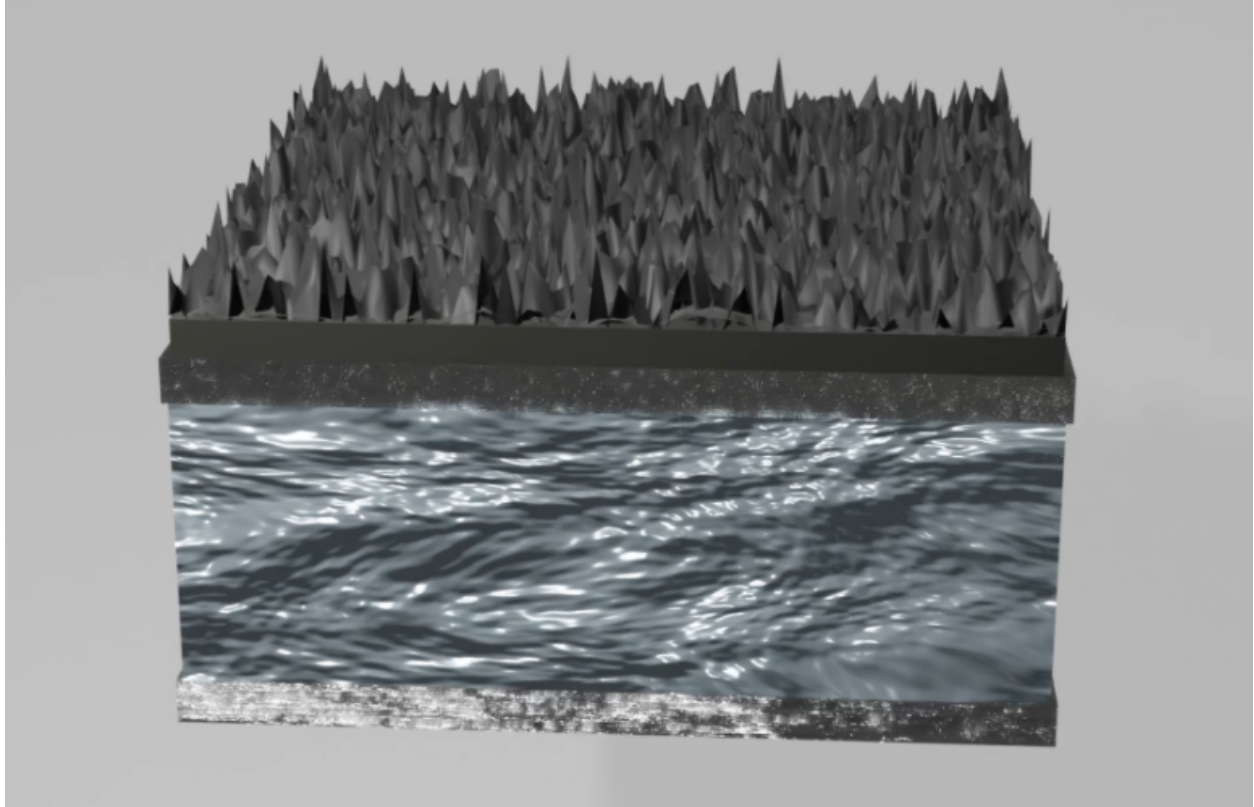


In this design, the C-14 can be stored in either the diamonds (102) embedded in the copper (103), or in the diamond which was deposited via chemical vapor deposition (105), and similarly to the last design, the electrons are emitted through the DLC (101), and then travel through a dielectric or a vacuum (106), before reaching an electron collection plate, where it can be stored for later

use. This allows for more storage of the C-14, which could potentially mean a longer lifespan. However, CVD is also a more expensive process.

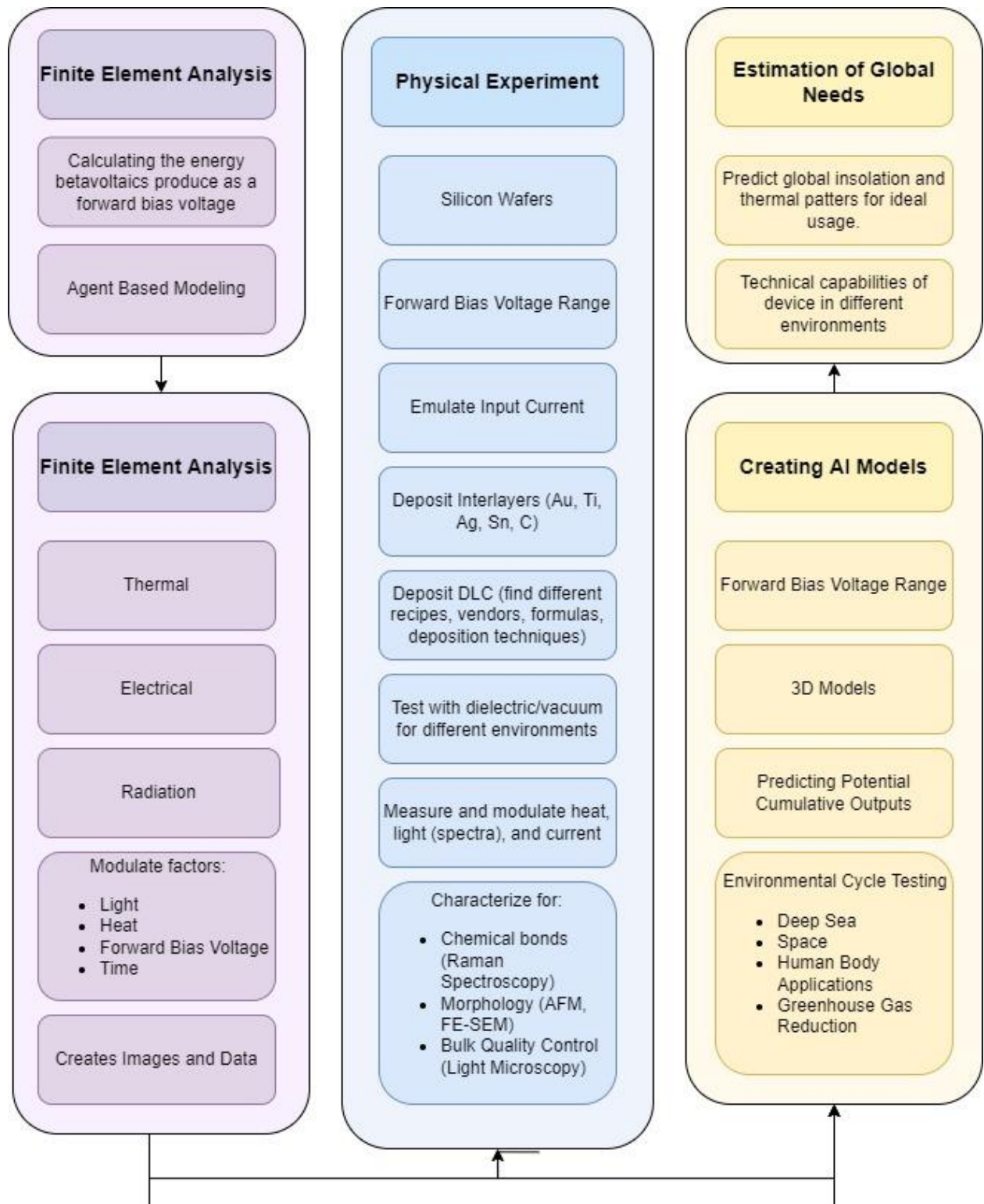


Sintered carbon species (103) was another design, where the C-14 could be stored. The carbon species would be made out of reused, or recycled materials. Out of all the processes, this one would be the cheapest, however, it also would be the least efficient. It would most likely be useful in areas that are less remote on Earth but would benefit from having a long-term energy resource that did not need to be replaced frequently.



*This is a 3D version of the initial conception of the device. *This is not to scale, the DLC coating in this design should be around 300-1000nm, whereas the wafers are roughly 500 um thick.*

Project Overview



A comprehensive workflow detailing the various experiments conducted this year

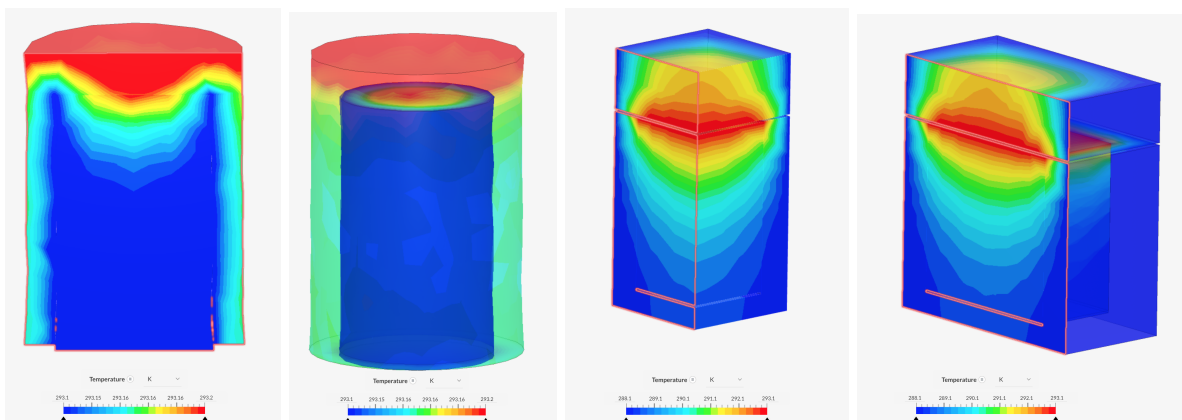
Control	Variables
Undoped silicon wafer	N-doped (phosphorus), P-doped (boron), DLC, DLC and chromium
STP	In a vacuum, Exposed to various temperatures
Sunlight or white LED visible light	Various spectra of light from monochromatic LEDs (300-1200 nm)
No forward-bias voltage	Forward bias voltage added (in a range of 10 steps approximating SOTA betavoltaics)
Full surround DLC coating	Single sided DLC coating, Abrasive removed/cleaved sides
DLC coating only	DLC coating with Chromium/Titanium interlayer

Simulations (Agent-Based Modeling, Finite Element Analysis)

Finite element method (FEM/FEA) analyses were also conducted to simulate both device performance under different conditions, as well as the performance of the integrated device, as a finalized, deployable product. Three software packages were used, focusing on different aspects

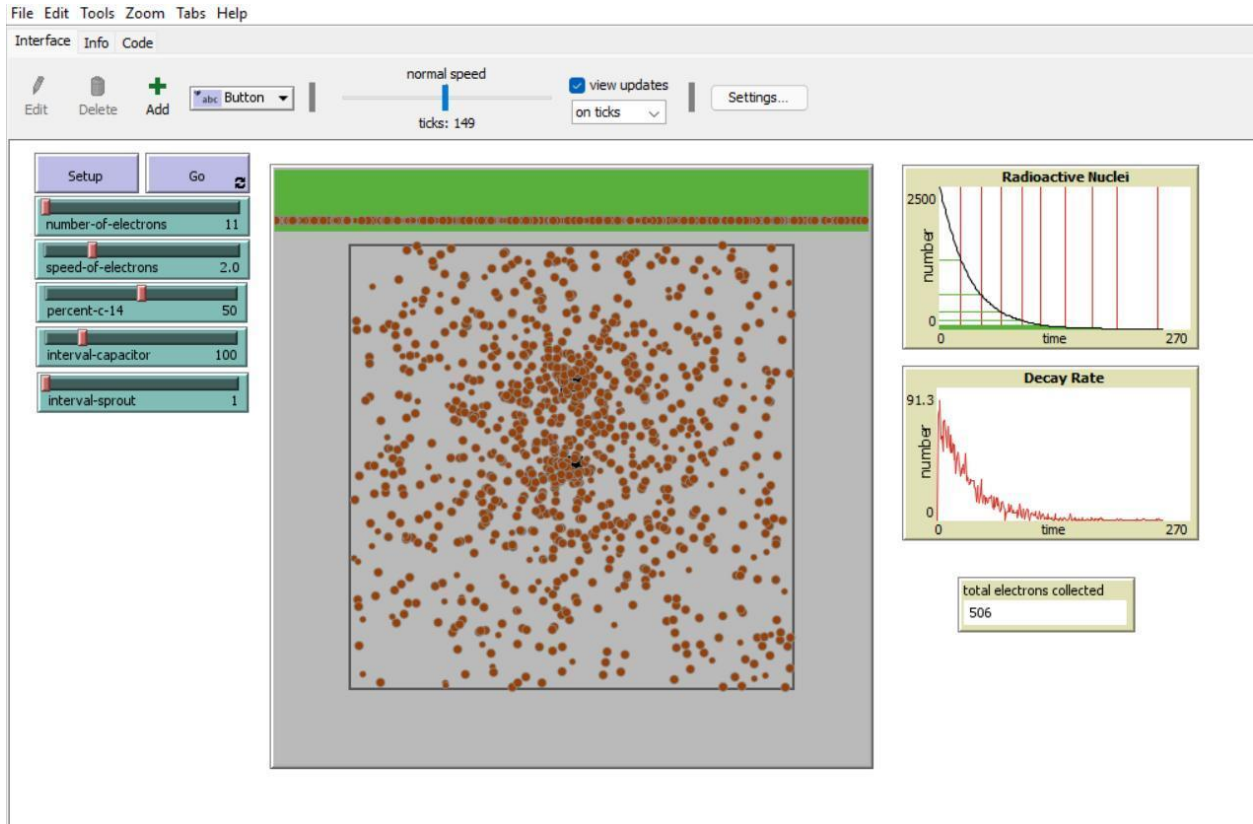
of the project including beta/blackbody radiation, the overall integrated system electrical and thermal performance, as well as heat flux, with a particular focus on predicting the potential thermionic effect of the DLC.

The FEA packages used included MSC Nastran/Patran (with the SINDA/G package from NASA for radiation predictions), as well as AutoFEM/AutoCAD (for the integrated system), and SimScale for thermal modeling. The finite element analysis was able to display the outputs showing the spread of the beta radiation, and the effects of including additional light and heat sources, as well as applying different amounts of forward bias voltages.



This figure shows the results of the simulated models for FEA.

Example of FEA output of a modeled DLC stacked composite substrate, showing internal heat radiating from a central point, in this case, a simulated betavoltaic source embedded in a composite substrate. This shows a quarter and half-section cutaway of the beta radiation source.

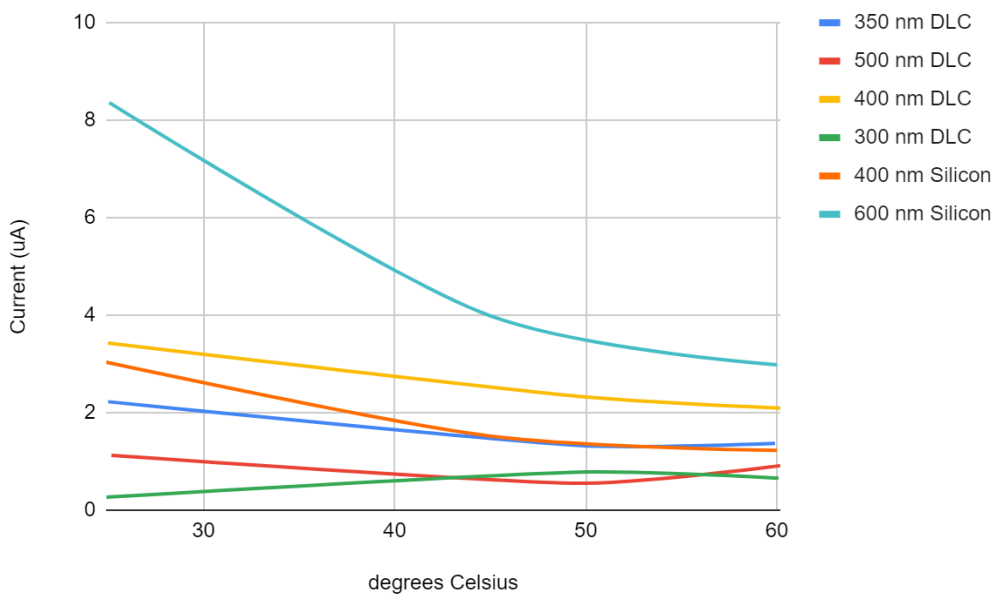


A screenshot of the agent-based modeling approach that was conducted, displaying the various sliding scales, as well as plots showing the current (in nanowatts) which was estimated to have been produced based on model constraints

Agent-based modeling using Netlogo was also conducted. This was done to emulate the output energy flux of the beta radiation sources, as well as maximum lifetimes of different configurations of the devices. Agent-based modeling was primarily conducted to demonstrate how the beta radiation would be spread throughout the different device configurations, both to predict performance values as well as to ascertain any potential safety hazards. Furthermore, this allowed for the identification of how many nanowatts of power would be able to be created due

to the C-14. This was done by designing the modeling system with input factors including the percent C-14 available to be emitted, and the total amount of atoms that might be in a single diamond crystal. A capacitor was also designed in this system, to collect electrons which would be stored, and then released at specific intervals (which could be specified). Through this system, the total amount of energy produced by the beta radiation, depending on the configuration and the number of C-14 in the system, could be calculated to find out how much energy would be available for the forward bias voltage.

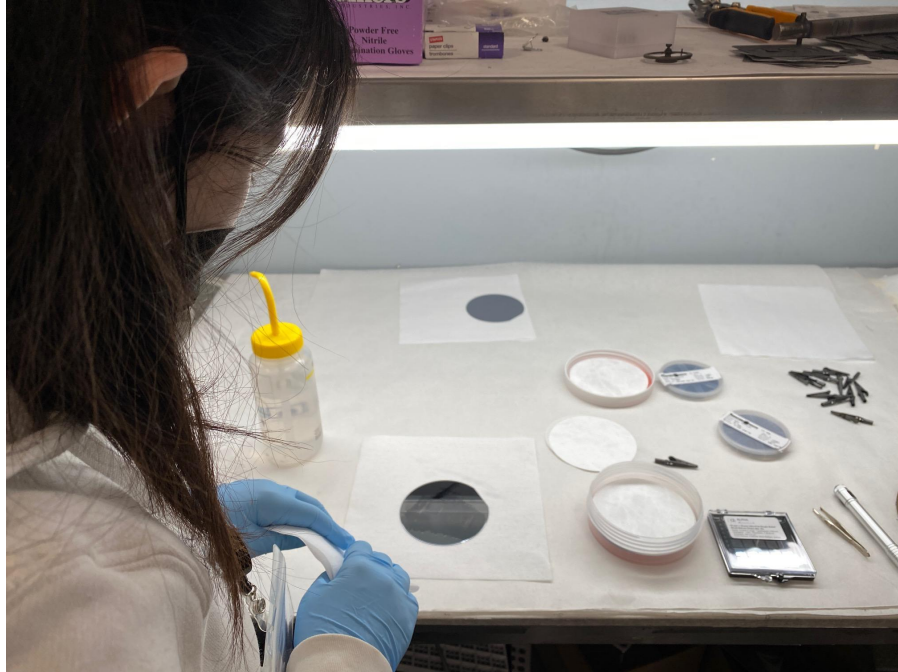
DLC Vacuum, Light, and Heat Modulation Experiments



The effect of temperature on the current produced by silicon and DLC solar cells

Physical experiments were also conducted through a number of different methods. First, 65 samples derived from silicon wafers and diamond copper composites were obtained by

contacting reclaimed wafer providers as well as other material suppliers in the semiconductor industry. A coating company in Kennebunk, Maine, Northeast Coating Technologies (NCT), was reached and provided support for this project, through free prep and coating services, for a range of silicon wafer samples, including N-type, P-type, and various crystal orientations of silicon wafers (100 and 111 types). NCT further provided the deposition of chromium interlayers as well as DLC coating on the surfaces of the wafer. In addition, a company in Taiwan (China Saw Abrasives Co) provided optical level DLC coated silicon wafers as well as copper-diamond composite samples as well. These samples were exposed to controlled light and heat sources. . Lighting sources were modulated both in terms of overall lumen output as well as wavelength (LED arrays were utilized for this), at a fixed distance from samples. Light intensity (lumens) were normalized via an Arduino-attached light sensor. Samples were tested in a vacuum setup using two levels of vacuum pump, that are connected to heating elements which would raise the temperature of the samples through both radiation, and conduction. This was done to test both the photovoltaics and the thermionic properties of the samples.



Working with the chromium coated silicon wafers, to be coated with DLC.



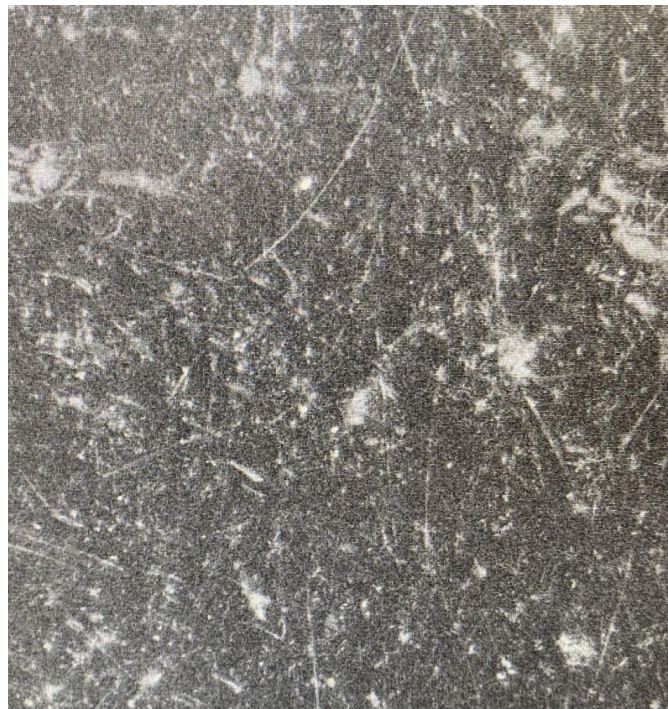
A fully-loaded batch of silicon wafers already coated with a chromium interlayer, ready to be coated with DLC.



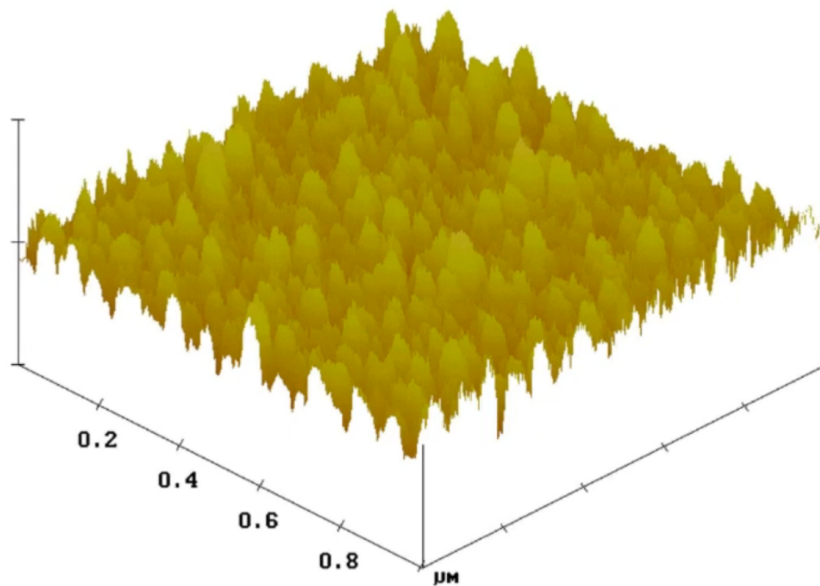
A sample of a silicon wafer coated with DLC, with traces placed on top. This is one of the completed samples, which were used for testing in various environments to test their efficiencies.



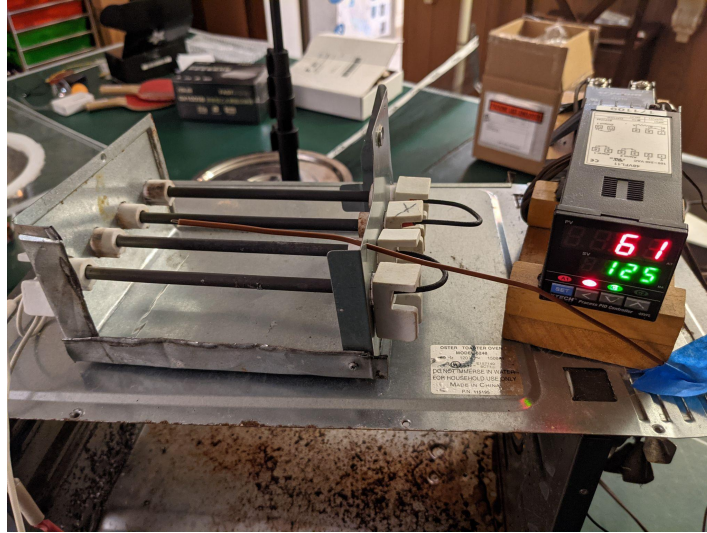
Imaging samples that were already coated with DLC under a scanning electron microscope (SEM) to observe the tip morphologies of the DLC.



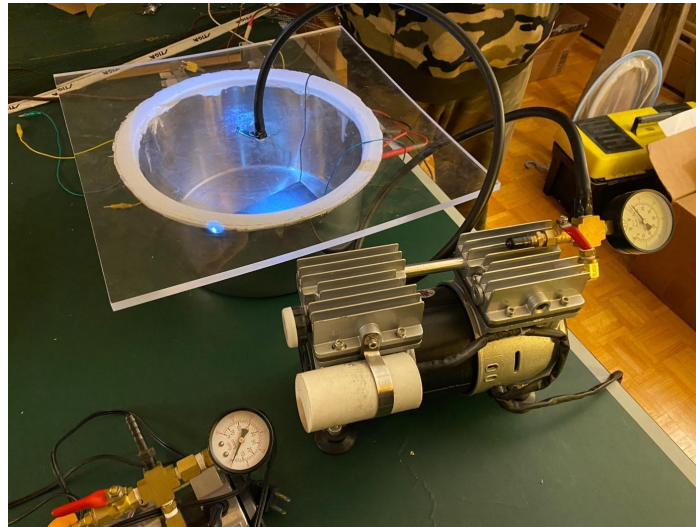
SEM micrograph showing the surface quality of one of my DLC on chromium specimens
Showing large scratch like features approximately 100um in length. Despite significant cleaning
in an ultrasonic bath as well as a 99 percent isopropanol bath there were still some surface
quality concerns. Micron sized scratches on the wafer surface may be affecting energy density of
the device and this may vary from sample to sample. It is therefore important to consider
overall surface quality after deposition as well as tip morphologies.



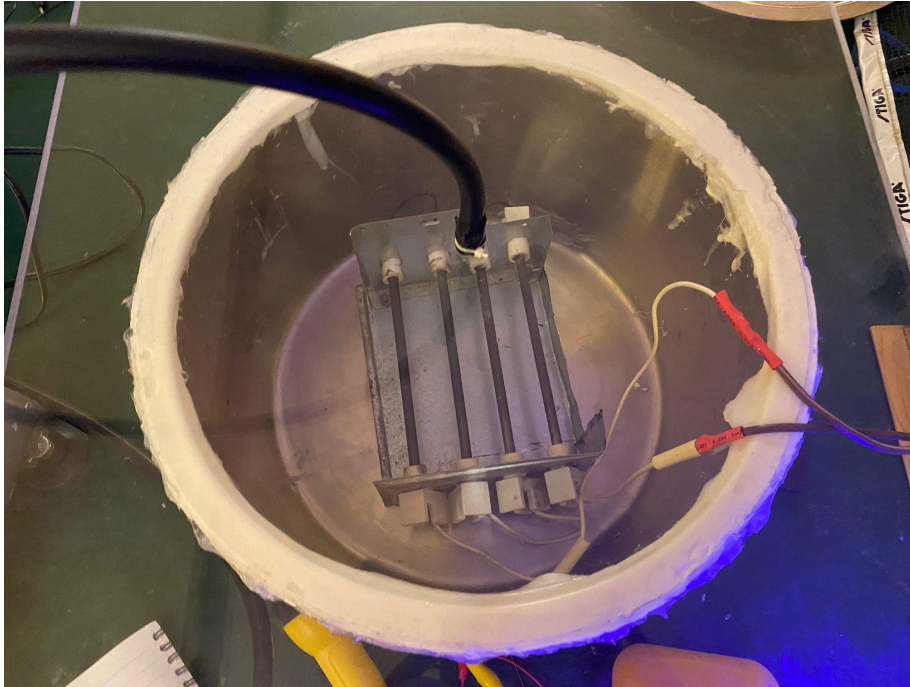
This is an AFM (Atomic force microscopy) micrograph of one of the samples provided to me,
showing clearly, the field emission tips with features as small as tens of nanometers, and as tall
as 200 nanometers, with a clear variation in overall morphology. It's assumed that the
morphology characteristics of the tips play a significant role in the capacity of the material to
emit electrons in both thermoelectric and photoelectric configurations.



A close up of the heating element which was designed, and maintained at a steady, constant temperature using a PID controller (proportional integral derivative)



The vacuum set-up was designed to withstand an excess of 75 mm Hg of pressure (as can be seen, the larger vacuum is currently reading ~70). The clear acrylic allows for photographic documentation of samples and viewing of the experiments.



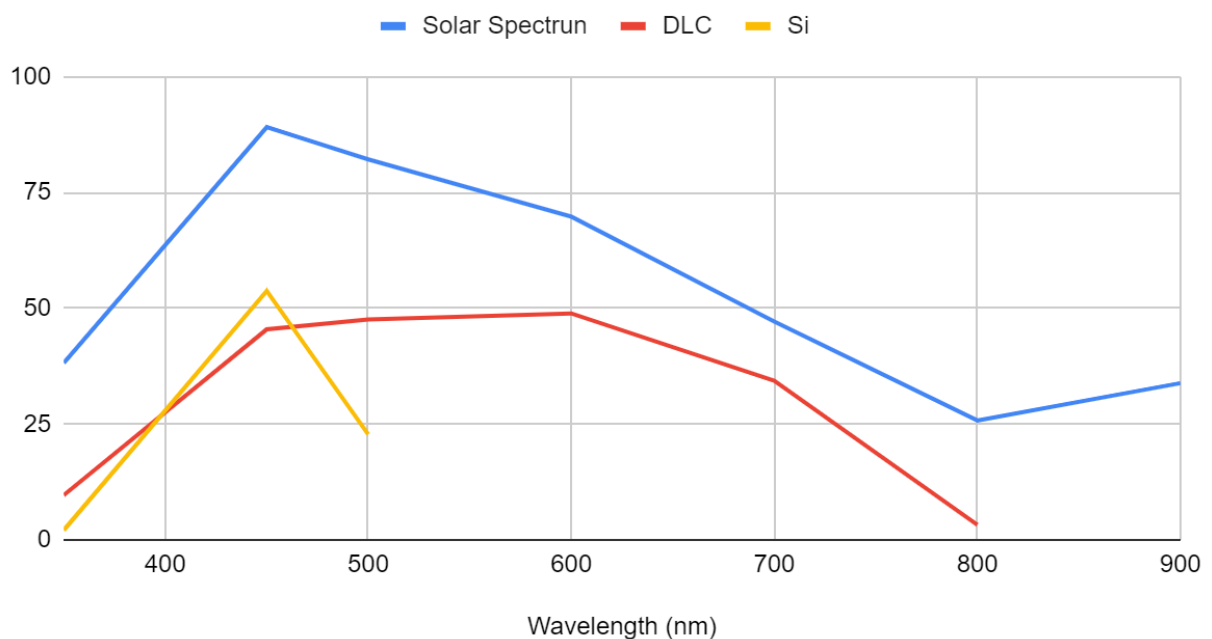
A heating element was tested inside the vacuum, to test how that would affect the samples.

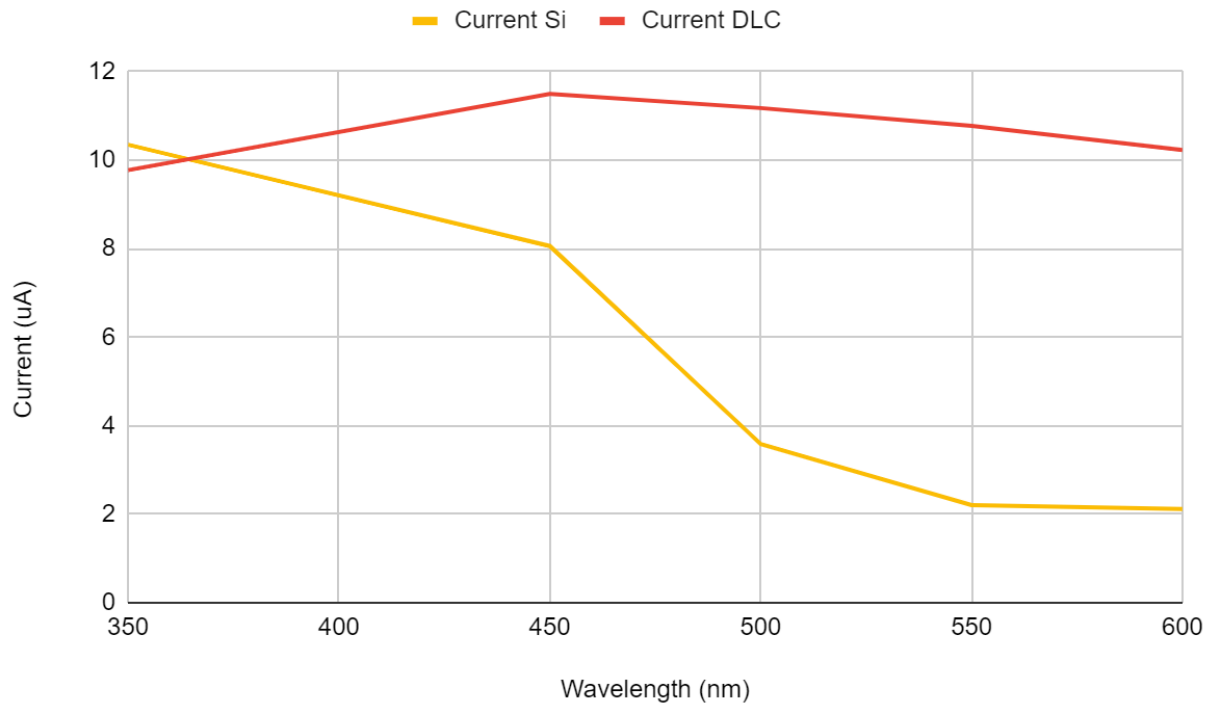
Spectral Response

Since fine-grained, specialized spectral absorption analysis equipment was unavailable during these experiments, a method was devised to replicate these analyses, with a lower level of granularity. However, it was felt that this approach would be sufficient for a first-order analysis, to ascertain the regions of best response in terms of wavelength-region specific energy output. A series of experiments were conducted, using a fixed array of calibrated diffused LEDs, with equal light output, at 12 different wavelengths, ranging from UV through near-infrared (~350-1200nm). Since typical silicon solar cells tend to respond well to visible light, this experiment was conducted to determine if there might be a spectral response shift, and/or if that

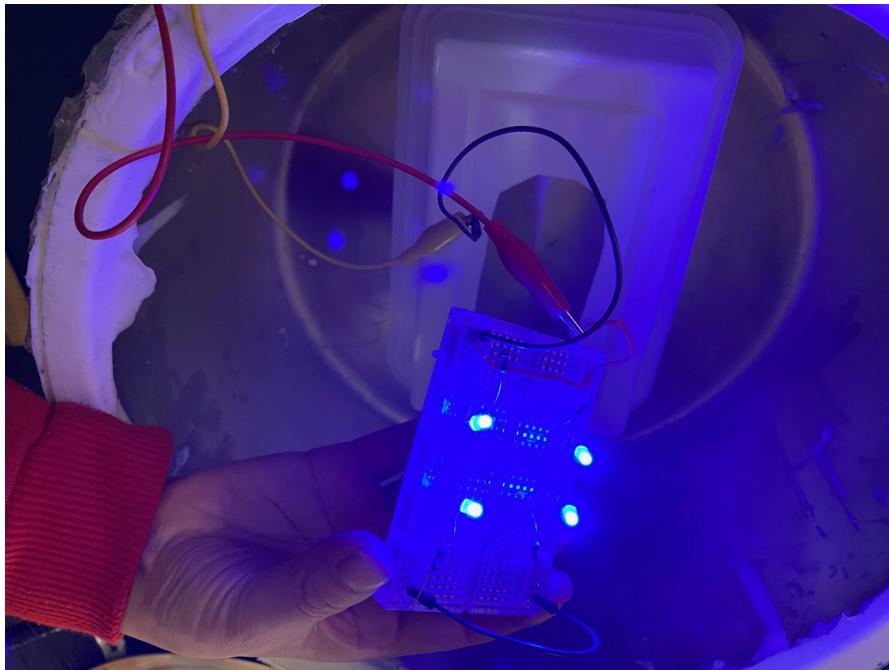
may be advantageous for certain potential operating conditions for the device. LED's tested included: 350, 450, 500, 550, 600, 700, 800, 850, 900, 1000, 1100, 1200 nm. This represented a combination of LED's which were already available, plus additional LED's purchased in the IR range, specifically for this experiment. LEDs were aligned in arrays of 4, and each array was replaced and positioned in the same location, for each test, to ensure that the same amount and position of light was used for each iteration. The absorption of infrared light using the DLC photovoltaics (at approximately 900 nm) resulted in nearly an order of magnitude greater energy efficiency compared to that of a traditional silicon solar cell.

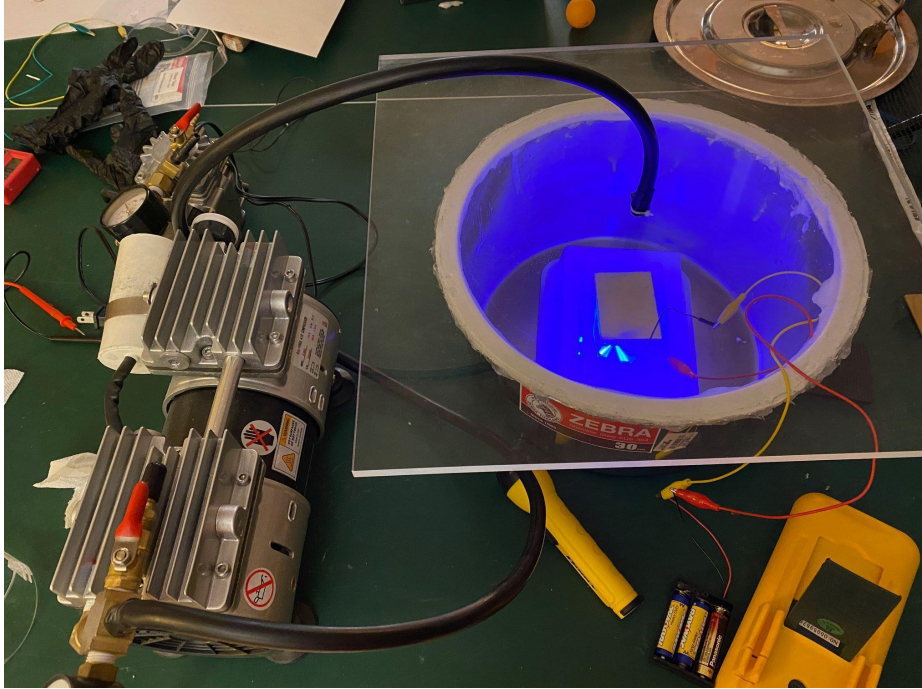
Solar Spectrum, DLC and Si





Comparing the spectral responses of DLC (in red) and Silicon (in yellow).





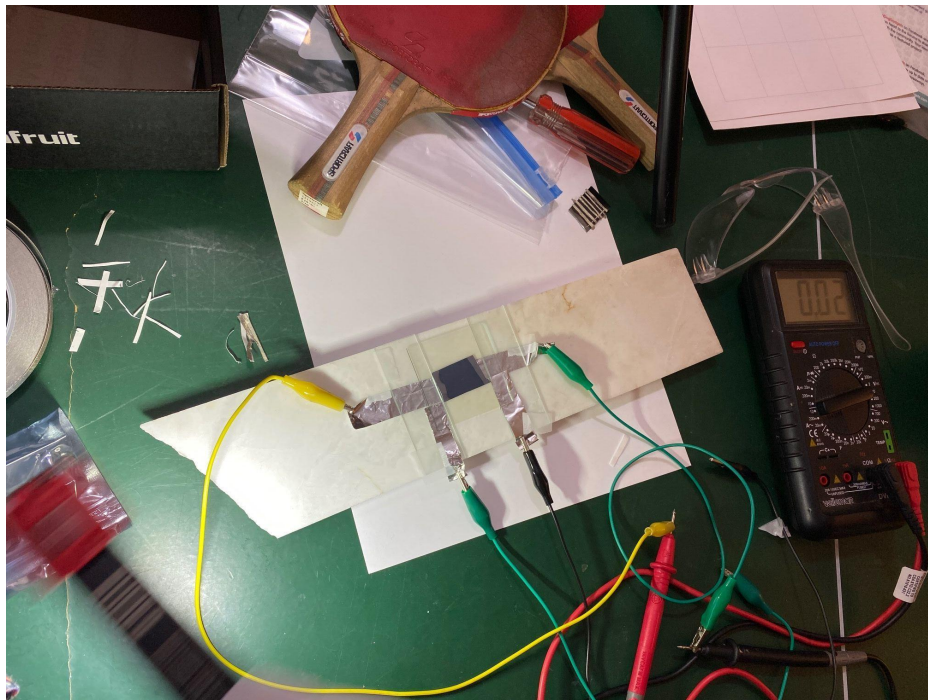


A close-up and more distant views of the spectral analysis set-up at various wavelengths of light, including 850 nanometers (which can be seen in the last figure)

Vacuum configuration using ITO Glass

ITO (Indium Tin Oxide) glass was used in the vacuum configuration of the device, as an alternative means of electron collection, as opposed to metal surface traces (in some experimental designs, conductive “maker tape” was used). ITO Glass is capable of collecting and transferring electrons, while at the same time permitting the substantial transmission of light, in both the visible and infrared spectra, allowing for greater extensibility of designs focusing primarily on the photovoltaic response of DLC. The vacuum configuration is utilized (emulating space/satellite applications) due to the fact that field emission of electrons from DLC field

emitter tips is substantially greater in a high vacuum, rather than standard sea level atmospheric conditions. Even extremely low voltages can arc when the electric field is strong enough, or a substantially high enough vacuum can be achieved. Maintaining a vacuum on the surface of Earth poses challenges and this problem is even greater in the deep ocean, however, a dielectric can be used in the place of a vacuum, for certain specific configurations. In a space environment, which is a natural vacuum, this field emission effect will be far easier to achieve, at a lower cost point, and with higher output energy densities. Furthermore, due to its radiation hardness, DLC will be ideal for this application, and is likely to maintain high efficiency energy production capabilities for a significantly longer duration, than silicon or other semiconductor substrates.



A close up of the ITO set-up.

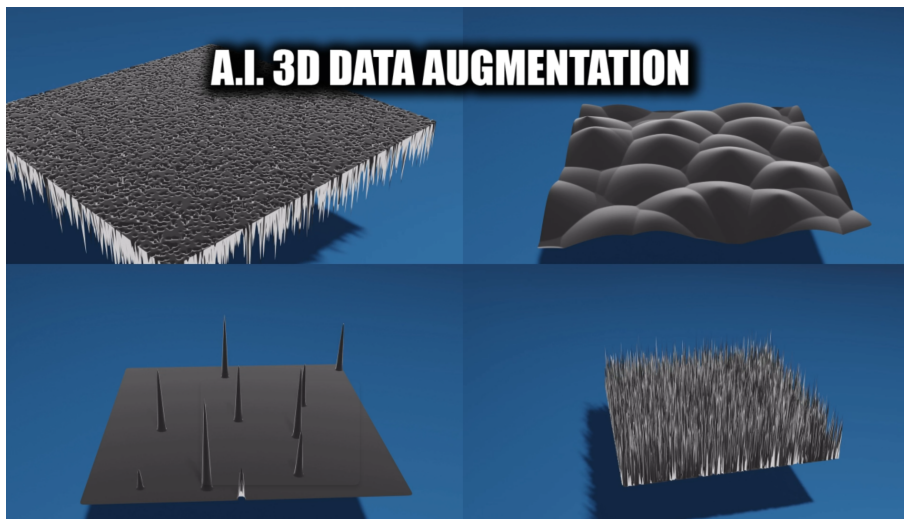
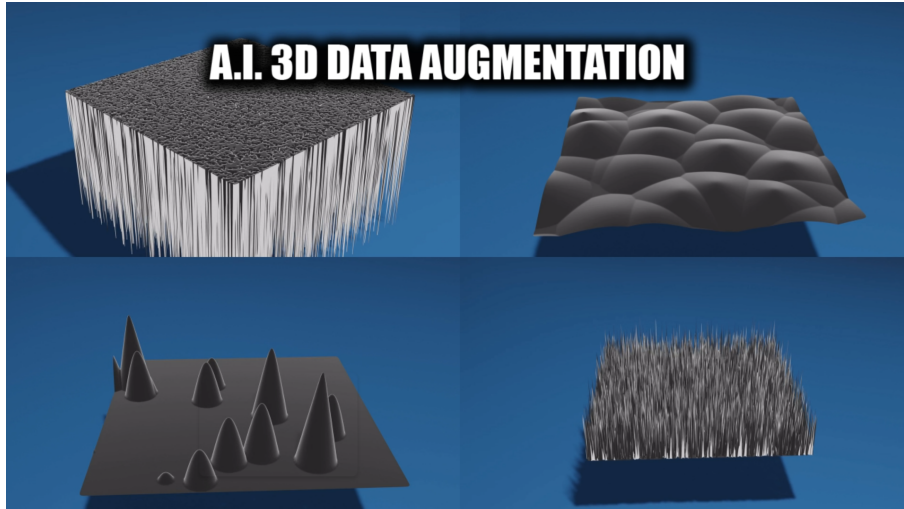
Betavoltaic Forward Bias Voltage Emulation

To emulate the potential benefits of a beta radiation source, to provide a forward bias voltage source for the system, particularly in vacuum-based space applications, a source of equivalent power was introduced. A current limiting circuit was created, and applied to a watch battery, to yield a 5mA, .5V output, which is a typical (approximate average) capability of a typical betavoltaic device, such as a tritium based device (as developed by betavoltaic companies such as Widetronix or Citylabs).

Convolutional Neural Networks

Convolutional Neural Networks (CNNs) were used to conduct a preliminary investigation into the ideal configuration of tip morphologies in various different environments and to find which would be the most energy-efficient under specified conditions. This was trained from numerous different sources, including relevant literature which contained data regarding similar topics, physical experiments that were conducted, as well as data that was augmented through using 3D CAD raytracing software, primarily the latest version of Blender, with an automated workflow to vary output geometries and generate a large sample of renders, using Blender-integrated Python. For the physical experiments, many trials of various different configurations were tested to obtain a range of 204 data points. Modulation of the physical prototypes included adjusting the thickness of the DLC coating, the sp³/sp² ratio, and the hydrogenation, as well as doping the silicon wafers with different elements (such as boron for p-type wafers and phosphorus for n-type wafers), and using different composites as the cell substrates. However, it is also assumed that the DLC field emission tip morphologies themselves play a substantial role in the energy

production capabilities of the material. Depending on deposition recipes used, different tip morphologies can result, and this can yield substantially different energy outputs. As such, it is important to study the localized differences in energy outputs, as compared to morphologies. Further, the surface condition of the substrate and the overall quality of the deposition and adhesion to the substrate interlayer play a major role in the ability of the DLC to produce quality results. As such, it is important to use image-based data to make these correlations, as opposed to reducing the data to geometric approximations and simply running attention-based RNN models. The use of SEM and AFM-derived image-based data, along with data augmentation, is important, to take into account not only tip morphology but the bulk quality of the deposition, in general. This data can then be used to correlate physical morphologies and DLC coating quality to energy density capabilities; in some cases, there are thermionic vs photovoltaic advantages to different geometries, and with additional funding and equipment access, further research in this promising area will be possible.



A few of the images showing what was used for the data augmentation, that was created with Blender

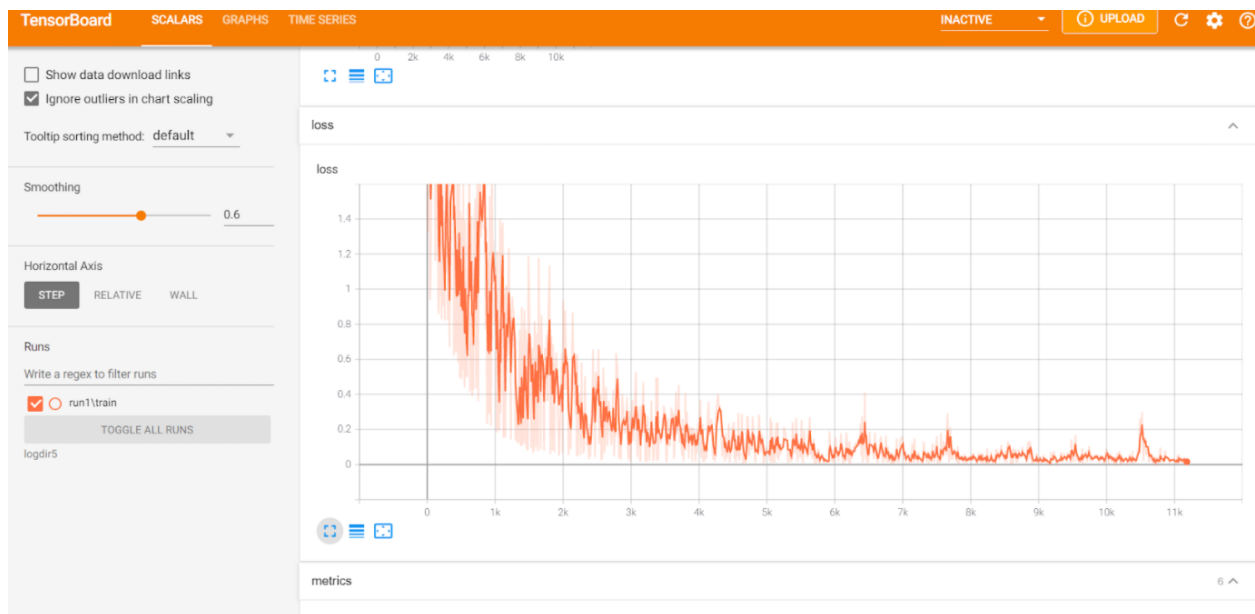
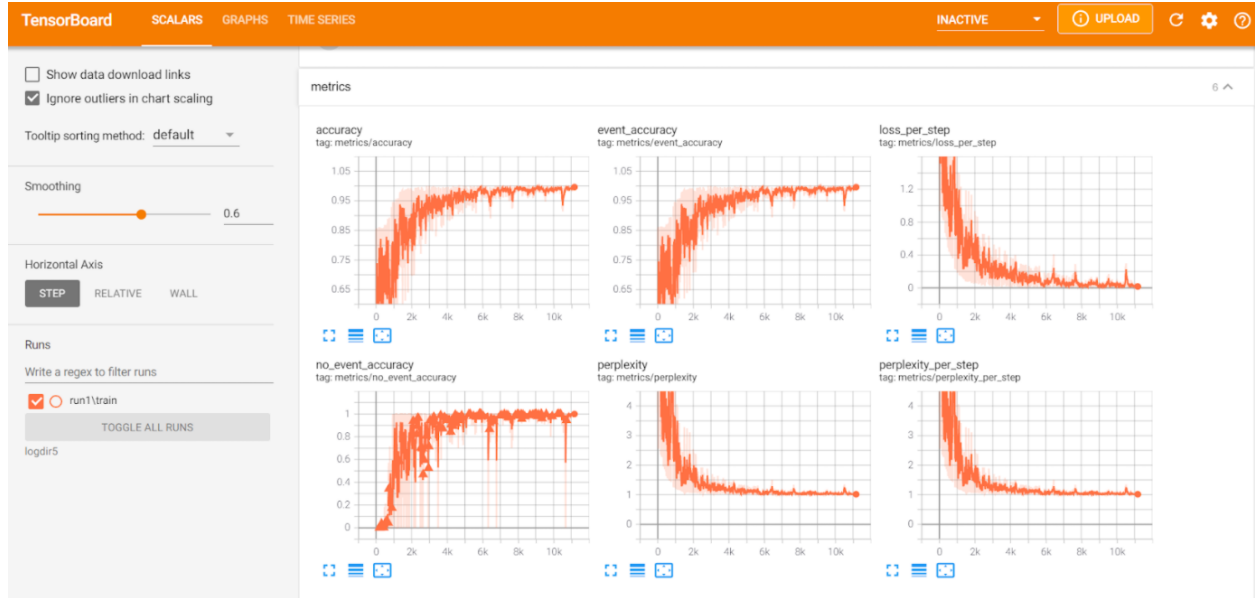
n=204	Predicted Accurate	Predicted Inaccurate	
Actual Accurate	TP = 95	FN = 14	109
Actual Inaccurate	FP = 11	TN = 84	95
	106	98	

A confusion matrix of the accuracy of the prediction, when testing the model with physical samples. The overall accuracy was roughly 88%.

Recurrent Neural Networks

Recurrent Neural Networks (RNNs) were used to predict how the device would operate under a multitude of environmental conditions, for preparation of usage in remote environments of extreme temperatures, aerospace applications, and also predict the sustainability and impact of this system will have on the environment. This was done using Tensorflow 2.7, within an Anaconda Python 3.8 environment. Training and testing data were collected via a combination of real-world data (from peer-reviewed journals, as well as output data from FEA/agent-based modeling simulations. ABM data was collected automatically from Netlogo, and over 1,000 data points per experiment were used.

The most efficient configurations for this device were studied, and determined based on the models that were generated. This includes switching the space in between the DLC and the electron collection plate with a vacuum or a dielectric, depending on the pressure exerted on the outside. For example, in space applications, there would simply be a vacuum between the DLC and the collection plate, whereas, in underwater remote applications, it would be filled with a dielectric.



Various metrics regarding the RNN models. The figure on the bottom displays the loss, which decreased significantly, demonstrating that the training was successful.

Results

FEA-informed ABM modeling with Netlogo yielded over 2,000 simulations, with multivariant data endpoints. This output was used in Tensorflow-Keras RNNs as training and testing data to feed an Attention model, to determine the likelihood of device configuration success. It was estimated that an N-type Si semiconductor base, with a Cr or Ti interlayer, as well as 200 nm (ranging from 80 to 400 in the ideal range) layer of DLC, ideally with a 60%+ sp³ content would achieve the best results.

Testing of DLC coated samples, both from the Taiwan and Maine provided batches yielded clear results. A demonstrable photoelectric effect was observed with DLC-coated N-type and undoped Si wafers. N-type Si wafers showed the strongest results with 50-80mV on most samples.

It was noticed that peak energies were obtained when the light was flashed on the samples briefly, potentially indicating that energy was dissipating, due to an insufficient method of electron collection.

Power Results Achieved

Type	Current Density	Voltage
Vacuum based configuration, with ITO glass electron collection	10^{-6} mA/cm ²	5×10^{-6} mV
Vacuum based configuration, with ITO glass electron collection with forward bias voltage	5×10^{-4} mA/cm ²	55 mV
P-N junction / conductive tape traces applied to surface of DLC	0.1mA/cm ²	102mV

Furthermore, it was demonstrated that a bias voltage across the substrate increased voltage output substantially.

When exposed to heat, thicker samples (up to 1.5 um from the NCT batch), we're able to demonstrate an increase (up to ~5%) in energy production, however, the gain in power output leveled off above 45°C.

When comparing the predicted vs ground-truth data gathered from testing, peer-reviewed publications (PRP) as well as linear regression (LR) based on this data, under different conditions, versus ABM (agent-based modeling) simulations, it was demonstrated that the simulations were valid and statistically significant, with a P of 3.83E-93.

t-Test: Paired Two Sample for Means

	<i>Testing, P.R.P. & L.R.</i>	<i>FEA-Informed A.B.M. Based Simulations</i>
Mean	0.739455882	0.79752322
Variance	0.004425737	0.018133922
Observations	204	204
Pearson Correlation	0.026868029	
Hypothesized Mean Difference	0	
df	203	
t Stat	-5.581675234	
P(T<=t) one-tail	3.78432E-08	
t Critical one-tail	1.652394461	
P(T<=t) two-tail	7.56864E-08	
t Critical two-tail	1.971718802	

Discussion and Conclusions

Results of simulated experiments (both ABM and FEA) demonstrated that a 5mm C-14 betavoltaic device configuration, in conjunction with a DLC semiconductor-type PN junction device could provide enough energy to power a small device for 20-30 years, at a theoretical higher voltage than the current capabilities of modern betavoltaics.

Furthermore, with the added benefit of power output enhancement using a forward bias voltage, in combination with the PN-junction design, it is estimated that this will substantially increase the power conversion capabilities as a supplement to both thermal and photon energy sources.

Certainly, the sp³/sp² ratio, the thickness of the film, the quality of the film, and the amount of hydrogen, nitrogen, and other contaminants all play substantial roles in the energy production capabilities of the material. However, it is assumed that emitter morphology also plays a significant role in the energy generation characteristics of the DLC films. Since the deposition formula for the DLC influences the morphology of the DLC emitter tips substantially, there is likely a significant amount of research that must be done to perfect the formula. Based on the variances in energy output (based on similar formulas) in peer reviewed sources, it can be assumed that there is another factor such as tip morphology, that likely plays a role, and could be leveraged to achieve significantly higher efficiencies. It was demonstrated in spectral analysis, that DLC was able to absorb a much wider range of wavelengths, beyond the visible spectrum and into the infrared wavelengths, than the conventional silicon photo cell.

While the ITO-vacuum configuration version of the device, tested in this project demonstrated relatively low current density and voltage, it is expected that this could be improved substantially

in a high vacuum environment, or the perfect vacuum of deep space. This, combined with diamond's radiation hardness, would make it an ideal configuration for space applications. The solid-state PN-junction design would be ideal for Earth-bound applications.

DLC can be deposited using extremely low-cost deposition technologies, and with the advent of new large-area deposition technologies and new low temp, large area plasma-enhance PVD systems, this cost is decreasing rapidly. As such, with system improvements and a lower cost substrate, it is estimated that the cost per Watt using a DLC device could potentially reach the level of photovoltaics. With improvements in electron collection and spacing between the ITO and DLC films in the vacuum configuration, it is thought that substantially greater energy production yields can be harvested from DLC.

This novel system has great potential to dominate the ~\$400m global betavoltaics market in the near term, and with additional system improvements, can enable the growing AioT and other mobile markets in the near future, helping to achieve the world's remote energy and data collection needs, while considering the world's climate goals.

References

1. A nuclear battery based on silicon p-i-n structures with electroplating ^{63}Ni layer. (n.d.). Nuclear A nuclear battery based on silicon p-i-n structures with electroplating ^{63}Ni layer. (n.d.). Nuclear Engineering and Technology, 51(8), 1978–1982.
<https://doi.org/10.1016/j.net.2019.06.003>
2. Arregui Mena, J. D., Margetts, L., Evans, L., Griffiths, D. V., Shterenlikht, A., Cebamanos, L., & Mummery, P. M. (2016). The stochastic finite element method for nuclear applications. Proceedings of the VII European Congress on Computational Methods in Applied Sciences and Engineering (ECCOMAS Congress 2016).
<http://dx.doi.org/10.7712/100016.1975.9348>
3. Boron-doped diamond-like amorphous carbon as photovoltaic films in solar cell. (n.d.). Solar Energy Materials and Solar Cells, 69(4), 339–344.
[https://doi.org/10.1016/S0927-0248\(00\)00400-1](https://doi.org/10.1016/S0927-0248(00)00400-1)
4. Burns, P. (1982). The Measurement of Alpha, Beta, and Gamma Radiations.
5. Cloudylabs. (2013). Thermoelectric cloud chamber [1080p] [Video]. In YouTube.
<https://www.youtube.com/watch?v=XGNvAEtYZkw>
6. Conduction Band - An overview. (n.d.). ScienceDirect Topics.
<https://www.sciencedirect.com/topics/engineering/conduction-band>
7. Contributors to Wikimedia projects. (2021, November 25). Low-energy electron diffraction. Wikipedia. https://en.wikipedia.org/wiki/Low-energy_electron_diffraction
8. Contributors to Wikimedia projects. (2022a, January 12). Decay heat. Wikipedia.
https://en.wikipedia.org/wiki/Decay_heat

9. Contributors to Wikimedia projects. (2022b, February 4). Cost of electricity by source. Wikipedia.
[https://en.wikipedia.org/wiki/Cost_of_electricity_by_source#/media/File:20201019_Leveled_Cost_of_Energy_\(LCOE,_Lazard\)_-_renewable_energy.svg](https://en.wikipedia.org/wiki/Cost_of_electricity_by_source#/media/File:20201019_Leveled_Cost_of_Energy_(LCOE,_Lazard)_-_renewable_energy.svg)
10. Cu incorporated amorphous diamond like carbon (DLC) composites: An efficient electron field emitter over a wide range of temperature. (n.d.). *Physica E: Low-Dimensional Systems and Nanostructures*, 97, 120–125.
<https://doi.org/10.1016/j.physe.2017.11.004>
11. Diamond-Like Carbon - An overview. (n.d.). ScienceDirect Topics. Retrieved February 4, 2022, from
<https://www.sciencedirect.com/topics/materials-science/diamond-like-carbon>
12. Diamond-like carbon thin films by microwave surface-wave plasma CVD aimed for the application of photovoltaic solar cells. (n.d.). *Diamond and Related Materials*, 14(11–12), 1973–1979. <https://doi.org/10.1016/j.diamond.2005.09.030>
13. Field emission from amorphous diamond coated silicon tips. (n.d.). *Materials Science and Engineering: B*, 74(1–3), 184–187. [https://doi.org/10.1016/S0921-5107\(99\)00558-9](https://doi.org/10.1016/S0921-5107(99)00558-9)
14. File:Physical Vapor deposition (pvd).jpg. (2018, January 26). Wikimedia Commons.
[https://commons.wikimedia.org/wiki/File:Physical_Vapor_Deposition_\(PVD\).jpg](https://commons.wikimedia.org/wiki/File:Physical_Vapor_Deposition_(PVD).jpg)
15. File:PlasmaCVD.PNG. (2008, September 20). Wikimedia Commons.
<https://commons.wikimedia.org/wiki/File:PlasmaCVD.PNG>
16. File:P-n Junction.jpg. (2013, February 9). Wikimedia Commons.
https://commons.wikimedia.org/wiki/File:P-n_junction.jpg

17. Formation of backcontacts on diamond electron emitters. (n.d.). *Applied Surface Science*, 146(1–4), 245–250. [https://doi.org/10.1016/S0169-4332\(99\)00031-8](https://doi.org/10.1016/S0169-4332(99)00031-8)
18. Ghosh, B., Ray, S. C., Espinoza-González, R., Villarroel, R., Hevia, S. A., & Alvarez-Vega, P. (2018). Surface plasmon effect in electrodeposited diamond-like carbon films for photovoltaic application. *Chemical Physics Letters*, 698, 60–66. <https://doi.org/10.1016/j.cplett.2018.03.004>
19. Kan, M.-C., Huang, J., Sung, J. C., & Yau, B.-S. (2003, December 31). Thermionic emission of amorphous diamond and field emission of carbon nanotubes. Elsevier. https://www.researchgate.net/publication/222397372_Thermionic_emission_of_amorphous_diamond_and_field_emission_of_carbon_nanotubes
20. Kornberg, O., & Popok, D. (n.d.). New methods to solve for radiation from finite element modelers. https://tfaws.nasa.gov/TFAWS06/Proceedings/Thermal%20Systems%20Tools%20and%20Methods/Papers/TFAWS06-1025_Paper_Kornberg.pdf
21. Noyce, R. N. (1953, January 1). A photoelectric investigation of surface states on insulators. <https://dspace.mit.edu/handle/1721.1/12296>
22. Products. (2017, May 9). CityLabs. <https://citylabs.net/products/>
23. Single Crystals - An overview. (n.d.). ScienceDirect Topics. <https://www.sciencedirect.com/topics/physics-and-astronomy/single-crystals>
24. staff, S. X. (2020, September 4). A novel betavoltaic technology with dyes for better energy production. Phys.Org. <https://phys.org/news/2020-09-betavoltaic-technology-dyes-energy-production.html>

25. Surface plasmon effect in electrodeposited diamond-like carbon films for photovoltaic application. (n.d.). *Chemical Physics Letters*, 698, 60–66.
<https://doi.org/10.1016/j.cplett.2018.03.004>
26. Technology Inst, N. &. (2019). 2007 Cleantech conference and trade show
Cleantech 2007. CRC Press. <http://dx.doi.org/10.1201/9780429187469>
27. Thermionic Emission - An overview. (n.d.). ScienceDirect Topics. Retrieved February 4, 2022, from
<https://www.sciencedirect.com/topics/physics-and-astronomy/thermionic-emission>
28. Thermionic emission of amorphous diamond and field emission of carbon nanotubes. (n.d.). *Carbon*, 41(14), 2839–2845. [https://doi.org/10.1016/S0008-6223\(03\)00414-7](https://doi.org/10.1016/S0008-6223(03)00414-7)
29. Vedantu. (n.d.). P-N junction. Vedantu. Retrieved February 4, 2022, from
<https://www.vedantu.com/physics/p-n-junction>
30. Workshop on Simulation and Modeling for Advanced Nuclear Energy Systems. (n.d.).
https://science.osti.gov/-/media/ascr/pdf/program-documents/docs/Gnep_06_final.pdf